




A critical review on the contributions of chemical and physical factors toward the nucleation and growth of large-area graphene

M. H. Ani^{1,*}, M. A. Kamarudin² , A. H. Ramlan¹, E. Ismail¹, M. S. Sirat¹, M. A. Mohamed³, and M. A. Azam⁴

¹Department of Manufacturing and Materials Engineering, Kulliyah of Engineering, International Islamic University Malaysia, P.O. Box 10, 50728 Kuala Lumpur, Malaysia

²Centre of Molecular Materials for Photonics and Electronics (CMMPE), Department of Engineering, University of Cambridge, Cambridge CB3 0FA, UK

³Institute of Microengineering and Nanoelectronic, Universiti Kebangsaan Malaysia, Bangi, Malaysia

⁴Carbon Research Technology Research Group, Advanced Manufacturing Centre, Faculty of Manufacturing Engineering, Universiti Teknikal Malaysia, Melaka, Malaysia

Received: 23 September 2017

Accepted: 3 January 2018

Published online:

17 January 2018

© The Author(s) 2018. This article is an open access publication

ABSTRACT

Since the first isolation of graphene over a decade ago, research into graphene has exponentially increased due to its excellent electrical, optical, mechanical and chemical properties. Graphene has been shown to enhance the performance of various electronic devices. In addition, graphene can be simply produced through chemical vapor deposition (CVD). Although the synthesis of graphene has been widely researched, especially for CVD growth method, the lack of understanding on various synthetic parameters still limits the fabrication of large-area and defect-free graphene films. This report critically reviews various parameters affecting the quality of CVD-grown graphene to understand the relationship between these parameters and the choice of metal substrates and to provide a point of reference for future studies of large-area, CVD-grown graphene.

Introduction

Graphene is a unique carbon allotrope and has a distinct hexagonal shape with a carbon atom at each vertex. The idea of graphene was first proposed by Wallace, who suggested that it should be possible to obtain a 2D structure of carbon [1]. However, it took more than 60 years to experimentally obtain

graphene, which was first realized via extraction from graphite by Geim and Novoselov in 2004 [2]. Graphene has been cited as a “wonder material” due to its superior properties of high charge carrier mobility, high optical transmissivity, high tensile strength and excellent thermal conductivity, among others [3]. Due to these exceptional properties, researchers have been diligently studying graphene

Address correspondence to E-mail: mhanafi@iiium.edu.my

for various applications, such as field effect transistors (FETs), solar cells, organic light emitting diode (OLED) display technologies and sensors [4–7].

Due to limitations in the fabrication process of defect-free and high-quality graphene, most applications for graphene are still only achievable on the laboratory scale. The simplest way of producing graphene is mechanical exfoliation, as demonstrated by Geim and Novoselov using the Scotch tape technique. This technique provides the highest quality graphene, i.e., monolayer and defect free. However, this method is only applicable to small-area production. There are a variety of other methods for producing graphene aimed at achieving large-area and high-quality graphene growth. These methods include chemical exfoliation [2], electrochemical exfoliation [8, 9] chemical synthesis [10, 11] and thermal chemical vapor deposition (CVD) [12, 13], among which the CVD method is the most promising synthetic method.

This method can produce large-area, monolayer graphene and is one of the most established methods of producing graphene [9, 10, 14–16]. The CVD synthesis of graphene was pioneered by Reina et al. and has been shown to produce large-area, monolayer graphene [17]. Though the preparation of graphene by the CVD method was established in 2009 by Li et al. [18], there are various parameters that still need to be optimized to obtain high-quality graphene. This review article aims to summarize the various factors that affect the synthesis of graphene.

Mechanism of graphene growth via CVD

As explained previously, the CVD technique is one of the preferred methods of producing graphene due to its ability to produce high-quality, large-area graphene on various substrates while still maintaining a low production cost, which is attractive from the viewpoint of industry [19, 20]. Typically, metals such as copper (Cu), nickel (Ni), platinum (Pt) and gold (Au) are used as the catalyst [21–24]. The air in the chamber is first purged using an inert gas such as nitrogen or argon to remove impurities in the reactor. Next, the reaction chamber is supplied with the precursor gas, such as methane or ethane, which acts as the carbon precursor through thermal decomposition. The chamber is heated to a high temperature, approximately 1000 °C, and then cooled to room

temperature, where carbon deposits on the surface of the substrate to form graphene.

Deposition of graphene onto a substrate is very complex and it involves many reactions that proceed simultaneously which sometimes even compete against each other. It is easier to divide the reactions into two categories. First, gas-phase reactions occurring as the carbon source, usually hydrocarbon such as methane, undergo decomposition reactions to form various active species. Second, these reactive species adsorb onto the catalyst surface and undergo dissolution as well as further reactions which form graphene on the surface.

Several reports exist on the gas-phase decomposition or pyrolysis of methane for the deposition of carbon [25, 26]. These reports highlight the complex nature of the decomposition. At high temperatures, methane undergoes pyrolysis to form various molecules and radical species which then recombines to form heavier hydrocarbons such as tar and carbon. Many reaction models have been proposed, with the most detailed discussions on gas-phase kinetics including more than 900 reactions that involves above 200 species. Not all reactions during pyrolysis will lead to the formation of graphene as there are parallel reactions that form other heavier hydrocarbons which also compete for the source methane. Currently much research is in progress to provide a model that accurately simulates graphene growth from hydrocarbon gases.

Such species formed during pyrolysis as well as unreacted methane will then adsorb onto the catalyst surface at which point additional reactions will happen. Here, the growth mechanisms for graphene on metal substrates differ from metal to metal depending on a wide range of parameters. Dissociative adsorption of methane and other species could still happen at this point which forms more reactive species on metal substrate [27]. Dehydrogenation then occurs, leaving only the carbon species adsorbed on the metal surface. These carbon species then will diffuse on the metal surface which leads to the supersaturation of carbon atoms as portrayed by a metal–carbon solubility diagram in Fig. 1a [28]. The supersaturation happens when the solvus line was either horizontally crossed as carbon content increases at constant temperature under continuous hydrocarbon feed (isothermal growth) or vertically crossed at certain carbon concentration during

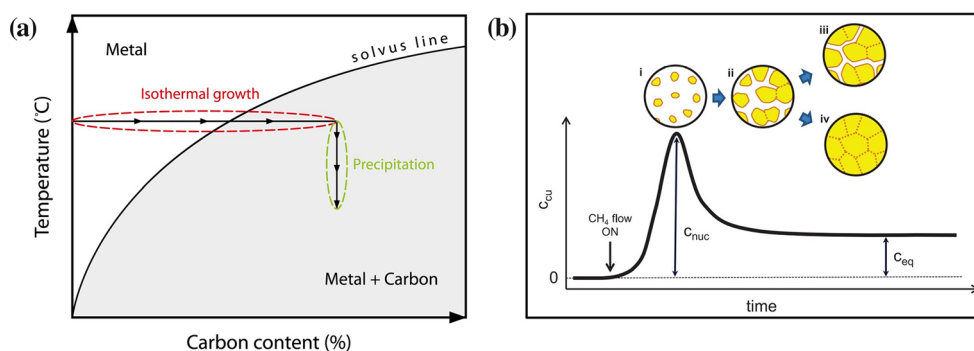


Figure 1 **a** Metal–carbon solubility diagram. **b** Detailed mechanism of graphene growth in CVD during isothermal growth process. [28] Published by The Royal Society of Chemistry.

cooling process which leads to reduction in carbon solubility (precipitation/segregation).

In isothermal growth, supersaturation of carbon atoms should reach a critical point (c_{nuc}) for graphene domain to nucleate and grow as shown in Fig. 1b [29]. Once carbon concentration level is lower than c_{nuc} , no new domains will be produced whereby only further growth of existing graphene domain will proceed. This growth process will proceed until supersaturated carbon has reached its equilibrium level (c_{eq}). Depending on the amount of supersaturated carbon left after the nucleation, the graphene domains will either coalesce to form a continuous polycrystalline film, or stop growing to produce partially covered graphene which could be controlled through the hydrocarbon gas concentration and exposure time.

Crystallinity and morphology of the substrates

Crystallinity

Properties of metallic substrates are greatly influenced by its bulk structure. Atomic arrangements determine the crystal lattice forming various planes which become the surface lattice orientation at the crystal surface. These lattice orientations play an important role in controlling the growth of graphene deposits.

In a detailed study by Wood et al. [30], the facet of the Cu structure was shown to affect the quality of the synthesized graphene. Graphene grown on Cu (111) tended to form a monolayer with few defects compared to graphene grown on Cu with other

Reprinted (adapted) with permission from [29]. Copyright (2017) American Chemical Society.

facets, and the growth rate was found to be faster [31, 32]. This is due to the Cu (111) crystal facet having a hexagonal shape similar to graphene, although Cu atoms are significantly larger than carbon atoms. There is a less mismatch of the two structures compared with other copper facets, which is approximately 3.8% for Cu (111) as opposed to 19.9% for Cu (100). The slight mismatch between the graphene layer and the underlying metal substrate was measured using an atomic Moiré interferometer [33]. Several Moiré patterns can be obtained depending on the crystallographic structure of the metal [34, 35]. In addition, Cu (111) has a lower surface energy than other Cu crystal orientations, and thus, monolayer and homogenous carbon nucleation are favorable on this surface [36]. Figure 2 shows the origin of the mismatch between graphene and the underlying metal crystal structure. The difference in the crystallographic orientation also allows, to some extent, a different growth mechanism, as in the case of Cu (111) where the growth of graphene is surface diffusion limited, whereas for Cu (100), monomer attachment to graphene is restricted [37]. The lattice mismatch can be calculated using the following equation (Eq. 1), which in the case of Cu (111) is written as

$$\left(\frac{\sqrt{3}a_{Cu}}{\sqrt{3}a_G} - 1 \right) \times 100 \quad (1)$$

where a_{Cu} is the Cu (111) lattice constant and a_G is the graphene lattice constant as defined by the Miller indices, as shown in Fig. 2 with the calculated values summarized in Table 1. However, reports have shown that annealing the copper substrate at high temperature changes its crystal structure [38]. It was

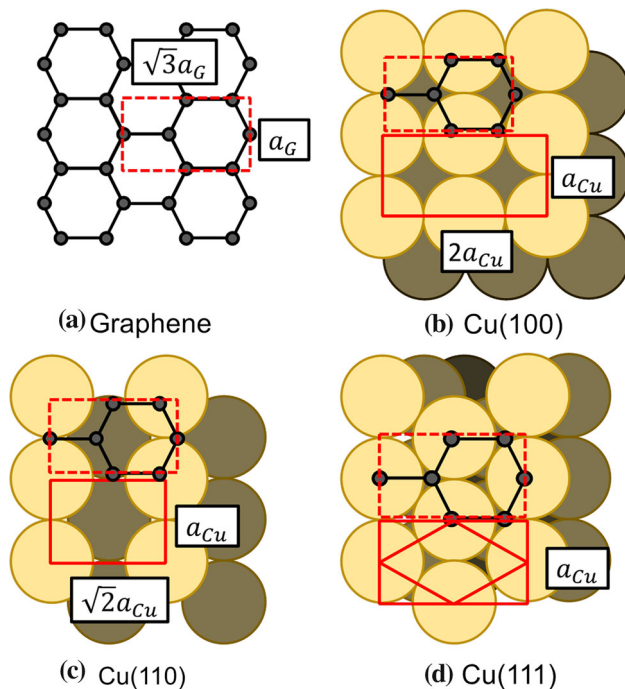


Figure 2 Comparison of the graphene unit cell and different copper crystallographic orientations. Adapted from [45], with the permission of AIP Publishing.

shown that at a temperature of up to 350 °C, Cu (111) is dominant, and upon increasing the temperature to 500 °C, the structure begins to change to Cu (100) [39]. This will inadvertently affect the quality of graphene during synthesis.

A similar observation was made for the Ni substrate, where the facet most similar to the Ni (111) orientation is homogeneously covered with fewer graphene layers compared to other facets, which is due to the lower binding energy on the Ni (111) crystal orientation and smaller lattice mismatch [40]. Table 1 summarizes the calculated lattice mismatch values for Cu, Ni and several other metals. It is believed that in the case of a metal alloy, the (111)

orientation is still the preferred metal surface for the growth of high-quality graphene, as it is still the lowest index facet [41]. However, Robinson et al. reported that the crystal orientation of Cu-Ni alloy changed from (110) to the midway between (100) and (111) after annealing [42].

During the synthesis of graphene, hydrogen gas is flowed through the furnace. Not only this gas is important for the formation of graphene but it also works to suppress the formation of different copper crystal facets. Liu et al. [46] reported that annealing the copper substrate in the presence of hydrogen reduces the possibility of forming the Cu (200) crystal structure, as opposed to annealing the substrate in the absence of hydrogen gas, as evidenced from the XRD data. The oxygen from CuO reacts with the hydrogen gas, forming water vapor when annealed at high temperature leaving behind metallic copper. Due to this reaction, the copper substrate reorganizes its structure to form a smoother and cleaner copper substrate, which allows for the growth of large-area graphene [47].

Early research on the CVD growth of graphene employed polycrystalline metals due to the lower cost of production. Polycrystalline substrates possess domains with different crystal orientations and hence grain boundaries that act as nucleation sites [48]. It has been shown that the graphene growth conforms to the structure of the grain boundaries, meaning that the more grain boundaries that a metal possesses, the smaller the size of the graphene domain and the more defects in the synthesized graphene [49].

Zhang et al. [50] performed a comparative study using single-crystalline and polycrystalline Ni substrates and found that more multilayer graphene is formed on the polycrystalline metal substrate than on the single-crystalline Ni substrate. This result was further supported by Bae et al. [51] who showed it is

Table 1 Summary of the graphene–metal separation and lattice mismatch

	Graphene–metal separation (nm) [43]	Lattice mismatch (%) [44]
Co (0001)	0.21	– 2.0
Ni (111)	0.21	– 1.2
Cu (111)	0.33	– 3.6
Ru (0001)	0.21	4.8
Pd (111)	0.25	3.2
Ag (111)	0.33	– 1.8
Ir (111)	0.34	4.6
Pt (111)	0.33	2.5
Au (111)	0.33	– 1.6

possible to prepare large-area, monolayer graphene via roll-to-roll processes and found that the graphene domain sizes correspond to the size of the grain boundaries. Notably, several other studies have shown the synthesis of single-crystal graphene on noble metals such as Pt and Ru [52, 53]. Figure 3 shows a schematic diagram representing the growth mechanism on single-crystalline and polycrystalline Ni substrates. Furthermore, it has been suggested that in the case of polycrystalline Ni substrates, the dissolution and segregation processes are inhomogeneous due to different crystal domains, and hence, multilayer graphene flakes are formed [54].

While single crystals could produce defect-free graphene, due to the high cost of producing single-crystalline metals, the growth of graphene on monocrystalline substrates is rather limited. However, research by Ago's group has shown that it is possible to grow single-crystalline metals on top of sapphire or MgO at a much lower cost, and graphene grown on these substrates was shown to be single-layer graphene [55, 56]. While cost could be drastically reduced by this epitaxial growth of single crystals, the increase in additional steps further adds to the complexity and time required for producing graphene.

In addition to graphene synthesis on single-crystal and polycrystal metal substrates, some studies have used liquid metal, which is in the amorphous form during the synthesis of high-quality graphene, despite the material lacking a crystal lattice [57, 58]. The formation of high-quality single-layer graphene results from the liquid metal providing a highly defect-free and ultra-smooth surface for graphene

growth [59]. The increased carbon solubility in liquid metal has also been cited as one of the factors that improve the formation of graphene [60]. As the distance between the atoms constantly changes, the space within the liquid metal also changes, allowing for the trapping of more carbon atoms. When the liquid metal cools, the surface starts to solidify, while the inside is still in the liquid phase, and hence, the carbon is homogeneously dispersed. The solidified surface of the liquid metal blocked the diffusion of carbon atoms and at the same time reduced the nucleation sites, thus forming a uniform layer of graphene at the surface [61]. This method is especially beneficial for metals with low carbon solubility, although it comes at the cost of extremely high temperature ($> 1100\text{ }^{\circ}\text{C}$) compared with the typical graphene growth temperature. The reaction rate of graphene on liquid metal has also been found to be very fast due to the movement of carbon being faster in a liquid than on a solid [62]. Figure 4 shows the schematic diagram of the carbon solubility in a metal for solid and liquid Cu.

Surface morphology

In addition to the crystal facet of the substrate, the surface morphology of the substrate is also an important parameter that influences the quality of graphene [63, 64]. It has been well established that the nucleation of carbon starts at regions containing defects, such as dislocations, grain boundaries and kinks. This is due to the defects and kinks having lower energy barriers for nucleation than the smooth surface [29]. Although the presence of nucleation

Figure 3 Schematic diagram showing the comparison of graphene growth on **a** single-crystalline and **b** polycrystalline Ni substrates. Adapted with permission from [54] by Springer.

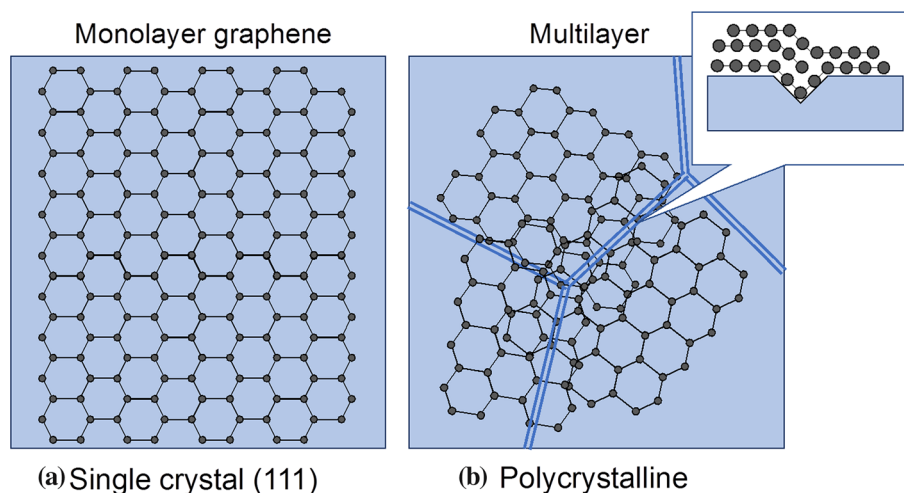
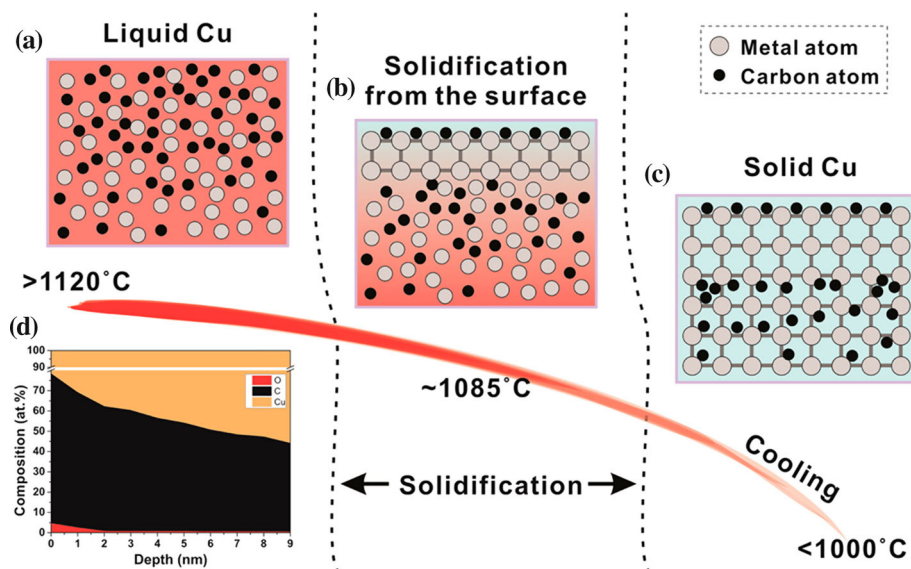


Figure 4 Schematic representation of the carbon solubility in liquid and solid Cu substrates. Reprinted with permission from [61]. Copyright (2017) American Chemical Society.



sites is necessary to initiate graphene growth, nucleation sites in the form of defects are not necessarily beneficial, as they tend to introduce defects in the graphene structure, leading to the formation of poor-quality graphene [65].

A study by Polat et al. [66] found that graphene synthesized on a smooth copper substrate was defect free and continuous compared to graphene synthesized on a rough substrate containing holes and cracks. Figure 5 compares the quality of graphene synthesized on smooth and rough copper substrates. It has been shown that when the CVD process is performed at low pressure, the surface morphology of the substrate plays an important role in determining the growth rate of graphene, as the sublimation of copper affects the desorption rate and nucleation rate [67].

The surface morphology of the substrate can be improved through electropolishing, which reduces up to 99% of the surface roughness and hence enhances the mechanical and electrical properties of the synthesized graphene [68]. Pre-treatment of the copper substrate, which includes pre-annealing the substrate in a hydrogen environment and etching with nitric acid, has been shown to remove impurities and modify the surface roughness [69, 47]. Pre-treatment results in an improved coverage of monolayer graphene.

In a simulation study using DFT, Gao et al. [70] showed that nucleation growth is preferred near the edge of the Ni substrate, rather than at the step, due to the significantly low energy barrier. Figure 6a

shows the nucleation rate at the terrace and step edge as a function of temperature. However, this is not applicable when the synthesis is performed on a very smooth substrate surface at high temperature. A detailed nucleation growth mechanism has been proposed which was derived from classical nucleation theory that showed that the nucleation rate of graphene at the terrace or step edge can be written using the following equation (Eq. 2)

$$R_{\text{nuc}} = J_0 \exp(-G^*/k_B T) \quad (2)$$

where J_0 is the nucleation rate pre-factor, G^* is the nucleation barrier, k_B is the Boltzmann constant and T is the reaction temperature [71]. Several other studies have observed similar results, where nucleation growth is more prevalent at the step edge than at the terrace [72, 73].

Figure 6b shows the nucleation rates on different defects, which act as nucleation sites, as a function of temperature. To achieve high-quality graphene, a low nucleation rate is preferable, which can be obtained at lower annealing temperature.

A direct way of reducing the nucleation density near the step edge of the substrate is by surface modification. Suzuki et al. [74] detailed a threefold atmospheric pressure CVD process that removes traces of Si impurities originating from the furnace and promotes the formation of wider terraces on Cu foils without having to change the CVD growth parameters. Zhang et al. developed a method for controlling the nucleation process on a CuO substrate by regulating the hydrogen flow in the furnace [75]. It

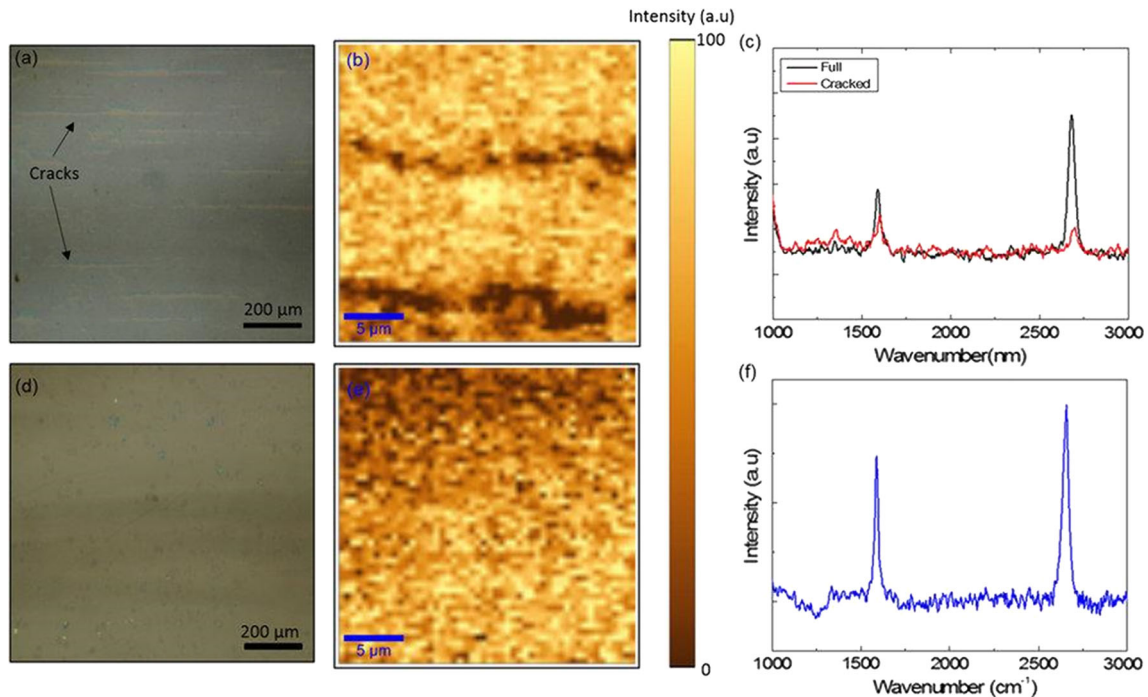
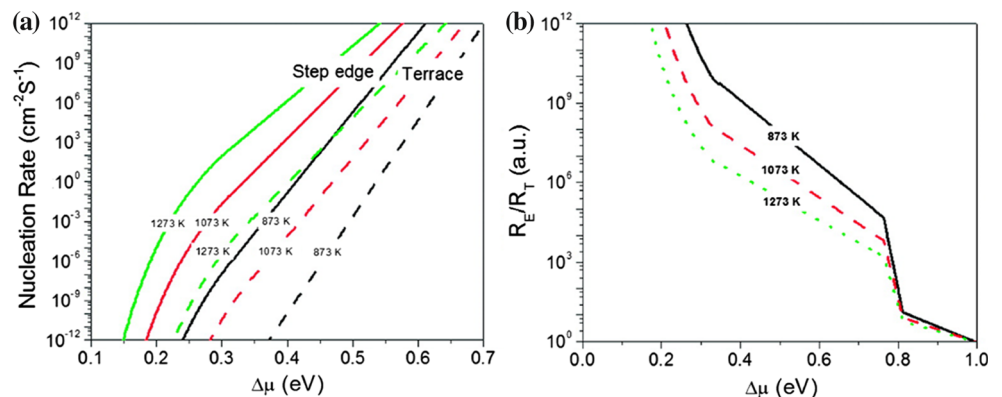


Figure 5 Graphene synthesized on **a** a rough Cu substrate and **d** a smooth Cu substrate and its resulting quality. Obtained from [66].

Figure 6 Nucleation rates of graphene at the terrace and step edge of a Ni substrate at different temperatures. Reprinted with permission from [70]. Copyright (2017) American Chemical Society.



has also been reported that oxygen can form oxide nucleation sites for graphene growth under high hydrogen partial pressures to produce single-layer graphene [76, 77]. The two-step CVD process proposed by Pham et al. [78] successfully realizes 5-mm-large graphene domains by separating the graphene nucleation and growth processes. The suppression of the nucleation process is attributed to the passivation of the active sites by oxygen, the lower energy barrier for the attachment of different graphene islands and the improved bulk diffusion of carbon within the copper bulk.

Alternatively, nucleation can be controlled by limiting the concentration of carbon used for growth.

In a very detailed study by Kraus et al. [79], controlling the carbon content in copper substrates was found to affect the nucleation growth and thus the quality of the synthesized graphene. There is also a report on the competition between graphene nucleation and hydrogen-induced etching, which starts at the nucleation site, as the site has a lower energy barrier [80]. This work lays the foundation for the synthesis of graphene with a desired morphology and shape. Another way of overcoming the issue of high nucleation density is through the use of a sandwiched Ni–Cu–Ni substrate, as shown by Ding et al. [81], where the nucleation sites on the Cu substrate can be selectively controlled. The perforated

top Ni substrate acts as a mask that allows the patterning of single-layer graphene due to Ni (higher carbon solubility) reducing the concentration of the carbon source, which in this case was CH_4 .

It is still possible to synthesize large-area graphene using polycrystalline metal substrates. One method of addressing this issue is through melamine pre-treatment of the polycrystalline Cu substrate, which suppresses the activation sites and thus controls the nucleation process [82]. Suppression of the nucleation density can also be achieved by mildly oxidizing the Cu substrate, resulting in reorganization of the nucleation sites for graphene growth [83]. Since graphene growth is governed by the size of the underlying crystal structure, it is also important to control the crystal domain size of the metal substrate [84]. Edwards et al. [85] published a review paper summarizing the different polycrystalline metal substrates that have been used to synthesize large-domain graphene. According to the paper, it is possible to synthesize graphene on a wide range of polycrystalline transition metal substrates. However, different synthetic conditions are required to obtain large-area graphene depending on the properties of the metal substrate.

It can be seen that the physical properties of the substrates greatly affects the growth of graphene. In physical terms, high-quality graphene growth favors a substrate that is very smooth and single crystalline in nature. The challenges in achieving this kind of physical properties are obvious in terms of time and cost. Therefore, a much feasible path forward is through the treatment of metal substrates by annealing and also surface pre-treatments to limit the defects that is caused by properties intrinsic to the crystallinity and surface morphology of the substrate.

Catalytic property, carbon solubility and substrate affinity

Another factor influencing graphene growth is the chemical properties of the metal substrates. Chemically, the metal substrates serve as a catalyst to promote the growth of graphene where without its presence, formation of graphene requires a large amount of energy, has a very slow formation rate or has a very low selectivity.

It might be beneficial to first discuss carbon–metal interactions. Carbon in the form of coal has long been

used in the steel industry. In a carbothermic reaction, carbon is used as the reducing agent to reduce metal oxides to pure metal [86]. In the case of copper (II) oxide, the oxide material is reduced to pure copper metal by carbon, producing carbon dioxide gas at the same time. The chemical reaction is given as follows (Eq. 3):



Calculating the Gibbs free formation energy shows that the value is negative, meaning that the reaction is spontaneous. This reaction requires high temperature to break the Cu–O bonds and form new C–O bonds. The reactivity of metal oxides to undergo carbothermic reaction can be determined from the Ellingham diagram (Fig. 7), which shows the stability of metal oxides as a function of temperature. The lower the position of the metal in the plot, the more stable the metal oxide, which means that NiO is more stable than CuO or Cu_2O . However, it possible to remove the oxide layer through reaction of the metal with carbon. The rate of reduction increases with temperature, as observed from the plot, as the slope is negative for the reduction reaction. The Ellingham diagram is a purely thermodynamics assessment and does not consider the reaction kinetics. Despite this phenomenon being well known in the steel industry, in the synthesis of graphene, this effect has not been considered. It would be prudent to investigate the interplay between the metal substrate and carbon when attempting to produce high-quality graphene.

While reduction in copper oxides by carbon is thermodynamically spontaneous, a report has demonstrated the formation of highly decoupled

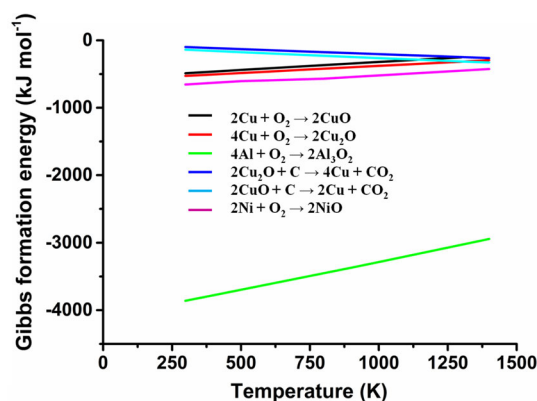


Figure 7 The Ellingham diagram showing the change in the Gibbs formation energy with temperature for different metal reactions. Graph plotted using the data obtained from [129].

graphene on copper oxide with good electronic properties [87]. This reduces the need to employ a complex graphene transfer process, which will incur extra costs in mass production. Nevertheless, the report did not mention the thickness of the oxide layer, which is also an important parameter since there is a limit to the carbon solubility in oxide materials. In addition, the presence of oxygen units on the surface of the copper substrate reduces the number of nucleation sites, which eventually allows for the formation of large graphene crystals, rather than small multi-domain graphene deposit [88]. However, a contradicting report states that oxygen units are preferable nucleation sites, citing the ease of carbon adsorption onto oxygen units on the copper surface [89]. This shows that the role of oxygen in the synthesis of high-quality and large-area graphene is still under debate and will remain an open-ended question for the foreseeable future. Nickel oxide has also been found to be advantageous for graphene synthesis, where a thin sub-oxide layer can reduce the graphene growth temperature down to 700 °C and promote the surface diffusion, rather than the bulk diffusion, of carbon atoms [90].

Another factor that affects the nucleation growth of graphene is the competing interaction between carbon–carbon (C–C) bonds and carbon–metal (C–M) bonds at the surface of the substrate at the graphene–metal interface [91]. The C–C bonds are responsible for the aggregation of carbon atoms, whereas the C–M bonds determine quality and structure of graphene. Comparison of C–C bond lengths on various metals calculated through *ab initio* method is summarized in Table 2. This comparison is a good indicator of whether C–C or C–M bonds will dominate during growth. C–C bonds have a length of 1.208 Å for a triple bond and 1.333 Å for a double-bonded carbon. C–C bonds of deposited carbon remain short if C–C bond dominates over C–M and gets longer when C–M bonds are more preferred than C–C bonds. Zhong et al. [92] investigated the nucleation growth on various metals and found that C–C interactions are strong on metals such as Au, Ag and Cu, while C–M interactions are stronger in the case of Ru, Rh, Ir and Pt.

It has been reported that Ni₃C is highly unstable and that Cu₃C does not exist due to the antibonding orbitals being filled and the splitting of the p orbitals of carbon being small [93]. On the other hand, transition metal carbides are several orders of

Table 2 C–C length on various substrates based on *ab initio* studies [92]

Metal substrate	C–C length (Å)
Ag	1.284
Au	1.297
Cu	1.302
Co	1.345
Ru/Pt	1.373
Rh	1.387
Ir	1.400

magnitude more stable than Ni₃C due to the presence of empty d shells, which allow for the formation of metal–carbide bonds [94]. Despite the strong interactions between transition metal and carbon atoms, it is still possible to synthesize graphene with high quality due to the suppression of carbon segregation and precipitation [95].

Another parameter related to the carbon affinity of metals is the carbon solubility, also known as the catalytic property of metals. The catalytic activity refers to the decomposition of hydrocarbons on metals. During the decomposition of hydrocarbons, activated carbon species are produced. These active species are responsible for lowering the activation energy for decomposition of the precursor gas. In other words, these active species affect the reaction temperature. As an example, graphene can be grown on a Pt substrate at temperatures as low as 750 °C, compared to the very high temperature of approximately 1000 °C required for graphene growth on a Cu substrate. Pt has a carbon solubility around 2% at 1000 °C [96]. This indicates that Pt substrates have a stronger catalytic ability for the dissociation of methane than Cu substrates [52]. From this fact, we can deduce that the lower the carbon solubility of a substrate, the weaker its catalytic ability for the dissociation of hydrocarbons. Pd substrates, similar to Pt, have a high carbon solubility around 4% at 1000 °C. Pd is well known for its “carbon-sponge” ability since it allows a very high amount of carbon diffusion [97]. The lower carbon affinity of Cu compared to other metal substrates is understandable, as catalytic activity occurs due to electron transfer from the C–H bonds to the 3d orbitals of the catalyst. Ni, for example, has two 3d unpaired electrons, while Cu has only one unpaired electron for the reaction [98].

Hence, the low reactivity of Cu is due to its filled electron shell, which is the most stable configuration.

This concept of isothermal growth only happens to low carbon solubility metal like Cu while additional precipitation process happen when the metal has larger amount of carbon solubility such as Ni. Due to the carbon solubility differences between Cu and Ni, the growth mechanism on these substrates differs with each other. In the case of a Ni substrate, carbon atoms dissolve and diffuse into the metal. As the temperature is reduced, the dissolved carbon atoms slowly segregate to the surface of the substrate due to the decreasing carbon solubility. The carbon atoms then diffuse to the surface of the substrate, where the carbon atoms attach to one another, forming a nucleation site that grows into graphene. However, in the case of the Cu substrate, the carbon atoms do not undergo the dissolution and segregation process. Studies using isotopic labeling have clearly shown the difference of the growth mechanism between metals high carbon solubility and low solubility [13]. Methane source with ^{12}C and ^{13}C was used alternately during deposition, and Ni shows graphene with both isotopes mixed due both carbons dissolving into the metal substrate. Whereas on Cu, graphene displays a distinct region as it can only grow from the only available carbon isotope. Figure 8 shows the different growth mechanisms of graphene on Ni and Cu substrates.

The carbon solubility of different metals at 1000 °C and the carbide formation energy are summarized in Table 3. The solubility of carbon in metals is governed by the following equation (Eq. 4):

$$S_P = S_{P_0} \exp\left(\frac{H_P}{k_B T}\right) \quad (4)$$

where S_{P_0} is the entropic pre-factor, H_P is the heat of precipitation, k_B is the Boltzmann constant and T is the absolute temperature [99].

To emphasize the importance of metal catalysts in graphene fabrication process, a review by Ning [101] highlighted various studies employing the direct graphene growth on dielectric substrates such as SiO_2 , alumina and diamond. It is crucial here to point out that although graphene is successfully grown on these dielectrics, the growth process requires the assistance of metal catalyst to enhance the carbon atoms diffusion on the substrate surface.

Previous accounts reported that growing graphene on dielectric substrates without metal catalyst proved

to be inefficient due to the very high pyrolysis temperature of the carbon precursor used [102–104]. For example, Kaplas et al. [105] apply the de-wetting ability of a pre-deposited Cu catalyst to facilitate carbon on a SiO_2 substrate. Using laser ablation method, the substrate surface is modified to change the melt pattern of the Cu catalyst thus resulting in the formation of rectangular, few-layer graphene without any transfer process.

Etching of Cu catalyst using acid has also been employed to produce graphene on dielectric substrates. Using commercial diamond substrate, Ueda et al. [106] annealed the Cu/diamond layers at 900–1000 °C under low pressure. Interestingly, this step resulted in the transformation of the diamond topmost layer to graphene through the catalytic effect of Cu. The Cu catalyst is then etched away by using diluted nitric acid.

Choi et al. [107] devised a unique experimental setup to grow single-layer graphene on SiO_2 substrate. In this study, a piece of rolled Cu is suspended above the substrate in a way that it is not in contact with each other. By doing this, the catalytic ability of the Cu foil can be utilized to grow graphene on SiO_2 without any transfer process.

Ni can also be used as catalyst for direct growth of graphene on dielectric substrate. Wang et al. [108] successfully grew graphene nano-ribbons on SiO_2 using shadow mask-assisted thermal evaporation. Graphene grown on Ni is then etched to remove the surface graphene film, leaving graphene micro-ribbons on the dielectric substrate.

Hart et al. [109] successfully produced graphene on SiO_2/Si substrate using cold-wall CVD. In this study, Ni and SiO_2 are stacked together prior to graphene growth. As carbon source is supplied, the carbon atoms will diffuse through the Ni crystal and along its grain boundaries. Then, the Ni layer is exfoliated using adhesive tape. They successfully produced graphene on SiO_2/Si substrate using cold-wall CVD. Ni and SiO_2 are stacked together prior to graphene growth. As carbon source is supplied, the carbon atoms will diffuse through the Ni crystal and along its grain boundaries. Then, Ni substrate is exfoliated mechanically using adhesive tape.

Thus, from the studies gathered, it is agreed that graphene growth on dielectric substrates requires metal catalysts to help lower the precursor gas dissociation temperature. Nevertheless, an exception can be made by using plasma-enhanced CVD as

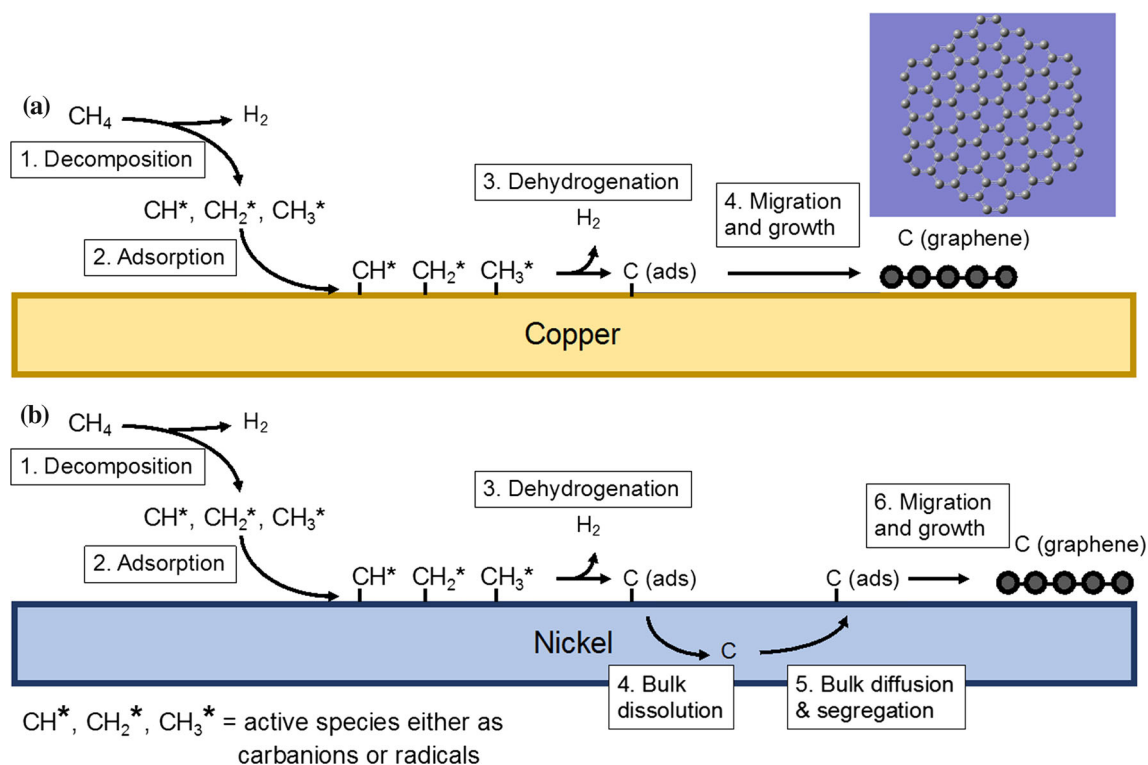


Figure 8 Schematic diagram of graphene growth on **a** copper and **b** nickel substrates. Adapted from [130].

Table 3 Carbon solubility and carbide formation energy of different metals

Metal	Carbon solubility at 1000 °C (at.%) [43]	Carbide formation energy (kJ mol ⁻¹) [100]
Co	3.41	- 10
Ni	2.03	- 5
Cu	0.04	21
Ru	1.56	- 4
Rh	0.89	0
Pd	5.98	5
Ag	0.01	33
Re	4.39	- 5
Ir	1.35	1
Pt	1.76	5
Au	0.01	37

reported by Munoz [110] and Jacob [111]. However, this study will not focus on that issue.

Bulk and surface diffusion

The kinetics and mechanisms of carbon diffusion into metal is a well-established area in the field of metallurgy. Bulk carbon diffusion depends on several

factors, including the carbon concentration, the structure and orientation of the crystal and temperature [112]. The bulk diffusivity of carbon into metals is also related to the carbon solubility. For a metal with low diffusivity, the carbon saturation is also low. Carbon will be accumulated on the surface of the metal, leading to the formation of multilayer graphene. Bulk diffusion is found to decrease with an increase in the dissolved carbon since there is a certain limit on how much a metal can contain carbon. A study by Wiltner et al. [113] has shown that for Ni substrates, the diffusion of carbon is improved along the (100) direction compared to the (111) crystal orientation. They explained that this is due to surface reorganization and the lower surface activation energy in the (100) direction [114]. The carbon solubility and thus diffusion can be affected by thermal annealing, where the formation of a barrier layer of oxide can suppress the diffusion of carbon in and out of the metal substrate [115]. Moshkalev et al. [116] determined that the shape of the catalytic substrate affects the solubility of the carbon atoms and the solubility is the highest on the arched surface and the lowest near the hollow surface. Using atomic modeling, Elliot et al. [117] found that at room

temperature, surface diffusion is much more preferable, whereas bulk diffusion occurs at high temperature.

Unlike bulk diffusion, which occurs due to the interstitial diffusion of carbon atoms throughout the host metal, surface diffusion occurs due to adatom adsorption at the interface of the metal. As the metal substrate cools, it shrinks in size, releasing trapped carbons to the surface of the metal. Surface diffusion is more important than bulk diffusion, as surface diffusion governs the domain size of the resultant graphene. This was reported by Hofmann et al. [118], who found that the energy barrier for surface diffusion is lower than that of bulk diffusion both in the case of Ni (111) and Co (111). Surface diffusion is also affected by the crystal facet, where certain crystal orientations are more favorable for diffusion. In the case of Cu, the preferential surface diffusion of carbon adatoms is in the Cu (111) direction due to the lower energy barrier [119]. This agrees with the previous section, which emphasized the favored (111) orientation of Cu in graphene synthesis. In the case of Si, which is an insulating material, despite the low carbon solubility, the diffusivity of carbon is rather high and can reach 10^{19} atoms cm^{-3} [120, 121]. It has been reported that the surface diffusion rate is higher than the bulk diffusion rate in Si [122]. After diffusing in Si to substitutionally form the SiC alloy at high temperature, the carbon atoms out diffuse to the Si surface, and then, segregation occurs to form graphene [123]. As expected for Si, the (111) orientation has a higher rate of diffusion than the (100) orientation due to the larger activation energy of carbon diffusion [124].

To evaluate the suitability of a metal to be used as a substrate, several parameters, such as the surface and bulk diffusivity, must be taken into account. These parameters affect the growth kinetics of the synthesized graphene. The diffusivity of carbon in metals is given by the following Arrhenius equation (Eq. 5):

$$D_T = D_0 \exp(-E_D/k_B T) \quad (5)$$

where D_T is the diffusion constant at temperature T , D_0 is the entropic pre-factor, E_D is the diffusion activation energy and k_B is the Boltzmann constant. The carbon diffusion length, L , can be determined from the following equation (Eq. 6):

$$L = 2\sqrt{D_T \tau} \quad (6)$$

where D_T is the carbon diffusion at temperature T and τ is the diffusion time [99]. A theoretical, comprehensive study by Yazyev et al. [125] derived the activation energy for different metals, which can be related back to the surface and subsurface diffusion of carbon atoms.

Changes in the metal composition through alloying also alter the graphene growth. Shin et al. reported that alloying Cu with Ag resulted in the diffusion of Ag into Cu, which altered the activation energy for the formation of graphene and at the same time suppressed multilayer nucleation [126]. Depending on the alloying ratio, the rate of nucleation or growth can be controlled by changing diffusivity of the C atoms, as in the case of the Cu–Ni alloy [127]. With an optimized Cu–Ni alloy ratio, the growth rate can be expedited while still maintaining the high quality of graphene, owing to the high carbon segregation rate in Ni and excellent catalytic properties of the alloy [128].

Conclusion

In this review, the various factors affecting the growth of large-area, monolayer, CVD-grown graphene were discussed. These factors are related to the physical and chemical properties of the substrate, which then determine the growth mechanism of the graphene film. Knowledge of the reaction parameters allows for the control of the graphene quality depending on the type of metal substrate. It can be concluded that the (111) crystal orientation is the favored crystallographic structure for all metals, as this orientation possesses the lowest activation energy regardless of the type of metal. In addition, the crystallinity, i.e., single crystalline or polycrystalline, of the catalyst affects the growth quality, where a single-crystalline catalyst results in a better graphene film. This is attributed to the growth mechanism of graphene, which tends to start near the grain boundaries and, since polycrystalline metals have many grain boundaries, the synthesized graphene will have a smaller domain size on top of a few layers.

Better control of the nucleation rate can be achieved through the use of a smooth surface with fewer defects, which is responsible for the growth of single-crystalline graphene. It has been shown that

defects and impurities can act as nucleation sites, thus improving the surface properties of the metal substrate, which is beneficial for graphene synthesis. The choice of metal will determine the quality of the synthesized graphene since different metals have a different carbon solubility, carbon affinity, bulk diffusion and surface diffusion. For a metal with low carbon solubility, it is ideal to have a low carbon affinity because higher affinity will result in the stable formation of carbide compounds, and thus, the formation of hexagonal graphene will be hindered. Surface diffusion affects the growth rate of graphene, where better surface diffusion tends to promote large-area growth and hence shorter reaction times.

As seen previously, despite the contradicting opinions on the effects of hydrogen gas on the quality of graphene, the advantages clearly outweigh the disadvantages of using hydrogen, either through the etching of graphene or the promotion of CH₄ decomposition. Although, excess hydrogen gas will have a deleterious result on the condition of the graphene sample. The effect of the cooling rate was also reviewed, where graphene formation will only begin when the temperature is low enough for a carbon atom to attach to another carbon atom. A faster cooling rate tends to produce few-layer graphene with high coverage, although too fast of a cooling rate will result in the formation of bilayer graphene. Overall, it is important to understand the growth mechanism to realize high-quality, single-layer graphene, and furthermore, it is clear that no one parameter is responsible for the synthesis of large-area graphene, but instead, a variety of different parameters are important.

Acknowledgements

This research was financially supported by the Ministry of Education, Malaysia, under Nanomite Program with Grant Number (LRGS15-003-0004).

Open Access This article is distributed under the terms of the Creative Commons Attribution 4.0 International License (<http://creativecommons.org/licenses/by/4.0/>), which permits unrestricted use, distribution, and reproduction in any medium, provided you give appropriate credit to the original author(s) and the source, provide a link to the

Creative Commons license, and indicate if changes were made.

References

- [1] Wallace PR (1947) The band theory of graphite. *Phys Rev* 71(9):622–634
- [2] Novoselov KS et al (2004) Electric field effect in atomically thin carbon films. *Science* 306(5696):666–669
- [3] Novoselov KS et al (2005) Two-dimensional atomic crystals. *Proc Natl Acad Sci USA* 102(30):10451–10453
- [4] Yin Z et al (2014) Graphene-based materials for solar cell applications. *Adv Energy Mater* 4(1):1–19
- [5] Pang S, Hernandez Y, Feng X, Müllen K (2011) Graphene as transparent electrode material for organic electronics. *Adv Mater* 23(25):2779–2795
- [6] Varghese SS, Lonkar S, Singh KK, Swaminathan S, Abdala A (2015) Recent advances in graphene based gas sensors. *Sens Actuators B Chem* 218:160–183
- [7] Raccichini R, Varzi A, Passerini S, Scrosati B (2015) The role of graphene for electrochemical energy storage. *Nat Mater* 14(3):271–279
- [8] Liu J (2017) *Graphene-based Composites for Electrochemical Energy Storage*, 1st edn. Springer Singapore, Singapore. <https://doi.org/10.1007/978-981-10-3388-9>
- [9] Yu P, Lowe SE, Simon GP, Zhong YL (2015) Electrochemical exfoliation of graphite and production of functional graphene. *Curr Opin Colloid Interface Sci* 20(5–6):329–338
- [10] Eigler S et al (2013) Wet chemical synthesis of graphene. *Adv Mater* 25(26):3583–3587
- [11] Stankovich S et al (2007) Synthesis of graphene-based nanosheets via chemical reduction of exfoliated graphite oxide. *Carbon* 45(7):1558–1565
- [12] Reina A et al (2009) Growth of large-area single- and Bilayer graphene by controlled carbon precipitation on polycrystalline Ni surfaces. *Nano Res* 2:509–516
- [13] Li X, Cai W, Colombo L, Ruoff RS (2009) Evolution of graphene growth on Ni and Cu by carbon isotope labeling. *Nano Lett* 9(12):4268–4272
- [14] Parvez K, Yang S, Feng X, Müllen K (2015) Exfoliation of graphene via wet chemical routes. *Synth Met* 210:123–132
- [15] Zhang Y, Zhang L, Zhou C (2013) Review of chemical vapor deposition of graphene and related applications. *Acc Chem Res* 46(10):2329–2339
- [16] Azam MA et al (2017) Review—critical considerations of high quality graphene synthesized by plasma-enhanced chemical vapor deposition for electronic and energy storage

- devices. *ECS J Solid State Sci Technol* 6(6):M3035–M3048
- [17] Reina A et al (2009) Few-layer graphene films on arbitrary substrates by chemical vapor deposition. *Nano Lett* 9(1):30–35
- [18] Li X et al (2009) Large-area synthesis of high-quality and uniform graphene films on copper foils. *Science* 324(5932):1312–1314
- [19] Nandamuri G, Roumimov S, Solanki R (2010) Chemical vapor deposition of graphene films. *Nanotechnology* 21(14):145604
- [20] Fang W, Hsu AL, Kong J (2015) A review of large-area bilayer graphene synthesis by chemical vapor deposition. *Nanoscale* 7(48):20335–20351
- [21] Oznuuer T, Pince E, Polat EO, Balci O, Salihoglu O, Kocabas C (2011) Synthesis of graphene on gold. *Appl Phys Lett* 98(18):183101-1–183101-3. <https://doi.org/10.1063/1.3584006>
- [22] Nam J et al (2017) Chemical vapor deposition of graphene on platinum: growth and substrate interaction. *Carbon* 111:733–740
- [23] Guermoune A et al (2011) Chemical vapor deposition synthesis of graphene on copper with methanol, ethanol, and propanol precursors. *Carbon* 49(13):4204–4210
- [24] Reina A et al (2009) Large area, few-layer graphene films on arbitrary substrates by chemical vapor deposition. *Nano Lett* 9(1):30–35
- [25] Hu C, Li H, Zhang S, Li W (2016) A molecular-level analysis of gas-phase reactions in chemical vapor deposition of carbon from methane using a detailed kinetic model. *J Mater Sci* 51(8):3897–3906. <https://doi.org/10.1007/s10853-015-9709-2>
- [26] Trinsoutrot P, Rabot C, Vergnes H, Delamoreanu A, Zenasni A, Caussat B (2014) The role of the gas phase in graphene formation by CVD on copper. *Chem Vap Depos* 20(1–3):51–58
- [27] Shibuta Y, Arifin R, Shimamura K, Oguri T, Shimojo F, Yamaguchi S (2013) Ab initio molecular dynamics simulation of dissociation of methane on nickel(1 1 1) surface: unravelling initial stage of graphene growth via a CVD technique. *Chem Phys Lett* 565:92–97
- [28] Cabrero-Vilatela A, Weatherup RS, Braeuninger-Weimer P, Caneva S, Hofmann S (2016) Towards a general growth model for graphene CVD on transition metal catalyts. *Nanoscale* 8(4):2149–2158
- [29] Kim H et al (2012) Activation energy paths for graphene nucleation and growth on Cu. *ACS Nano* 6(4):3614–3623
- [30] Wood JD, Schmucker SW, Lyons AS, Pop E, Lyding JW (2011) Effects of polycrystalline Cu substrate on graphene growth by chemical vapor deposition. *Nano Lett* 11(11):4547–4554
- [31] Cho J et al (2011) Atomic-scale investigation of graphene grown on Cu foil and the effects of thermal annealing. *ACS Nano* 5(5):3607–3613
- [32] Phan HD, Jung J, Kim Y, Van Ngoc H, Lee C (2016) Large-area single-crystal graphene grown on a recrystallized Cu(111) surface by using the hole-pocket method. *Nanoscale* 8:13781–13789
- [33] Miller DL et al (2010) Structural analysis of multilayer graphene via atomic moiré interferometry. *Phys Rev B Condens Matter Mater Phys* 81(12):1–6
- [34] Zeller P, Ma X, Günther S (2017) Indexing moiré patterns of metal-supported graphene and related systems: strategies and pitfalls. *New J Phys* 19(1):13015
- [35] Zeller P, Günther S (2014) What are the possible moire patterns of graphene on hexagonally packed surfaces? Universal solution for hexagonal coincidence lattices, derived by a geometric construction. *New J Phys* 16:083028-1–083028-29. <https://doi.org/10.1088/1367-2630/16/8/083028>
- [36] Skriver HL, Rosengard NM (1992) Surface energy and work function of elemental metals. *Phys Rev B* 46(11):7157–7168
- [37] Wu P, Zhang Y, Cui P, Li Z, Yang J, Zhang Z (2015) Carbon dimers as the dominant feeding species in epitaxial growth and morphological phase transition of graphene on different cu substrates. *Phys Rev Lett* 114(21):1–5
- [38] Du S, Li Y (2015) Effect of annealing on microstructure and mechanical properties of magnetron sputtered cu thin films. *Adv Mat Sci Eng* 2015:1–8
- [39] Demakov SL, Loginov YN, Illarionov AG, Ivanova MA, Karabanalov MS (2012) Effect of annealing temperature on the texture of copper wire. *Phys Met Metallogr* 113(7):720–726
- [40] Kozlova J, Niilisk A, Alles H, Sammelseg V (2015) Discontinuity and misorientation of graphene grown on nickel foil: effect of the substrate crystallographic orientation. *Carbon* 94:160–173
- [41] Liu X et al (2011) Segregation growth of graphene on Cu–Ni alloy for precise layer control. *J Phys Chem C* 115:11976–11982
- [42] Robinson ZR et al (2012) Substrate grain size and orientation of Cu and Cu–Ni Foils used for the growth of graphene films. *J Vac Sci Technol S* 30(1):011401(1)–011401(7)
- [43] Dahal A, Batzill M (2014) Graphene–nickel interfaces: a review. *Nanoscale* 6(5):2548
- [44] Gong C, Lee G, Shan B, Vogel EM, Wallace RM, Cho K (2010) First-principles study of metal-graphene interfaces.

- J Appl Phys 108(12):123711-1–123711-8. <https://doi.org/10.1063/1.3524232>
- [45] Shin HJ et al (2013) Influence of Cu crystallographic orientation on electron transport in graphene. *Appl Phys Lett* 102(16):163102-1–163102-5
- [46] Liu J, Adusumilli SP, Condoluci JJ, Rastogi AC, Bernier WE, Jones WE (2015) Effects of H₂ annealing on polycrystalline copper substrates for graphene growth during low pressure chemical vapor deposition. *Mater Lett* 153(August):132–135
- [47] Ibrahim A, Akhtar S, Atieh M, Karnik R, Laoui T (2015) Effects of annealing on copper substrate surface morphology and graphene growth by chemical vapor deposition. *Carbon* 94:369–377
- [48] Iwasaki T, Park HJ, Konuma M, Lee DS, Smet JH, Starke U (2011) Long-range ordered single-crystal graphene on high-quality heteroepitaxial Ni thin films grown on MgO(111). *Nano Lett* 11(1):79–84
- [49] Kanzaki K, Hibino H, Makimoto T (2013) Graphene layer formation on polycrystalline nickel grown by chemical vapor deposition. *Jpn J Appl Phys* 52:1–8
- [50] Zhang Y et al (2010) Comparison of graphene growth on single-crystalline and polycrystalline Ni by chemical vapor deposition. *J Phys Chem Lett* 1(20):3101–3107
- [51] Bae S et al (2010) Roll-to-roll production of 30-inch graphene films for transparent electrodes. *Nat Nanotechnol* 5(8):574–578
- [52] Gao L et al (2012) Repeated growth and bubbling transfer of graphene with millimetre-size single-crystal grains using platinum. *Nat Commun* 3:699
- [53] Yoshii S, Nozawa K, Toyoda K, Matsukawa N, Odagawa A, Tsujimura A (2011) Suppression of inhomogeneous segregation in graphene growth on epitaxial metal films. *Nano Lett* 11(7):2628–2633
- [54] Zhang Y et al (2012) Different growth behaviors of ambient pressure chemical vapor deposition graphene on Ni(111) and Ni films: a scanning tunneling microscopy study. *Nano Res* 5(6):402–411
- [55] Hu B et al (2012) Epitaxial growth of large-area single-layer graphene over Cu(1 1 1)/sapphire by atmospheric pressure CVD. *Carbon* 50(1):57–65
- [56] Vo-Van C et al (2011) Epitaxial graphene prepared by chemical vapor deposition on single crystal thin iridium films on sapphire. *Appl Phys Lett* 98(18):18–21
- [57] Geng D et al (2012) Uniform hexagonal graphene flakes and films grown on liquid copper surface. *Proc Natl Acad Sci* 109(21):7992–7996
- [58] Wang J et al (2013) High-mobility graphene on liquid p-block elements by ultra-low-loss CVD growth. *Sci Rep* 3:2670
- [59] Yan P, Jeong YJ, Islam MF, Pistorius C (2016) Real time and in situ observation of graphene growth on liquid metal surfaces via carbon segregation method using high-temperature confocal laser scanning microscope. *RSC Adv* 6:101235–101241
- [60] Geng D et al (2014) Controlled growth of single-crystal twelve-pointed graphene grains on a liquid Cu surface. *Adv Mater* 26(37):6423–6429
- [61] Zeng M, Tan L, Wang J, Chen L, Rummeli MH, Fu L (2014) Liquid metal: an innovative solution to uniform graphene films. *Chem Mater* 26(12):3637–3643
- [62] Ding G et al (2013) Chemical vapor deposition of graphene on liquid metal catalysts. *Carbon* 53:321–326
- [63] Han GH et al (2011) Influence of copper morphology in forming nucleation seeds for graphene growth. *Nano Lett* 11(10):4144–4148
- [64] Nie S, Wofford JM, Bartelt NC, Dubon OD, McCarty KF (2011) Origin of the mosaicity in graphene grown on Cu(111). *Phys Rev B Condens Matter Mater Phys* 84(15):155425-1–155425-7
- [65] Luo Z et al (2011) Effect of substrate roughness and feedstock concentration on growth of wafer-scale graphene at atmospheric pressure. *Chem Mater* 23(6):1441–1447
- [66] Polat EO, Balci O, Kakenov N, et al (2015) Synthesis of large area graphene for high performance in flexible optoelectronic devices. *Sci Rep* 5:16744. <https://doi.org/10.1038/srep16744>
- [67] Vlassioux I et al (2013) Graphene nucleation density on copper: fundamental role of background pressure. *J Phys Chem C* 117(37):18919–18926
- [68] Griep MH, Sandoz-Rosado E, Tumlin TM, Wetzel E (2016) Enhanced graphene mechanical properties through ultra-smooth copper growth substrates. *Nano Lett* 16(3):1657–1662
- [69] Kim MS, Woo JM, Geum DM, Rani JR, Jang JH (2014) Effect of copper surface pre-treatment on the properties of CVD grown graphene. *AIP Adv* 4(12):127107-1–127107-8
- [70] Gao J, Yip J, Zhao J, Yakobson BI, Ding F (2011) Graphene nucleation on transition metal surface: structure transformation and role of the metal step edge. *J Am Chem Soc* 133(13):5009–5015
- [71] Jiang D, Chen Z (2013) Graphene chemistry: theoretical perspectives. Wiley, New York
- [72] Morita M, Norimatsu W, Qian HJ, Irle S, Kusunoki M (2013) Atom-by-atom simulations of graphene growth by decomposition of SiC (0001): impact of the substrate steps. *Appl Phys Lett* 103(14):141602-1–141602-4
- [73] Garlow JA, Barrett LK, Wu L, Kisslinger K, Zhu Y, Pulecio JF (2016) Large-area growth of turbostratic graphene on

- Ni(111) via physical vapor deposition. *Sci Rep* 6(111):19804
- [74] Suzuki S, Nagamori T, Matsuoka Y, Yoshimura M (2014) Threefold atmospheric-pressure annealing for suppressing graphene nucleation on copper in chemical vapor deposition. *Jpn J Appl Phys* 53(9):095101
- [75] Zhang H et al (2016) Realizing controllable graphene nucleation by regulating the competition of hydrogen and oxygen during chemical vapor deposition heating. *Phys Chem Chem Phys* 18:23638–23642
- [76] Wang H, Wang G, Bao P, et al (2012) Controllable synthesis of submillimeter single-crystal monolayer graphene domains on copper foils by suppressing nucleation. *J Am Chem Soc* 134(8):3627–3630. <https://doi.org/10.1021/ja2105976>
- [77] Liu J et al (2015) Controllable growth of the graphene from millimeter-sized monolayer to multilayer on Cu by chemical vapor deposition. *Nanoscale Res Lett* 10(1):455
- [78] Pham PHQ, Zhou W, Quach NV, Li J, Zheng JG, Burke PJ (2016) Controlling nucleation density while simultaneously promoting edge growth using oxygen-assisted fast synthesis of isolated large-domain graphene. *Chem Mater* 28(18):6511–6519
- [79] Kraus J, Böbel M, Günther S (2016) Suppressing graphene nucleation during CVD on polycrystalline Cu by controlling the carbon content of the support foils. *Carbon* 96:153–165
- [80] Luo B, Gao E, Geng D, Wang H, Xu Z, Yu G (2017) Etching-controlled growth of graphene by chemical vapor deposition. *Chem Mater* 29(3):1022–1027
- [81] Ding D, Solís-Fernández P, Hibino H, Ago H (2016) Spatially controlled nucleation of single-crystal graphene on Cu assisted by stacked Ni. *ACS Nano* 10:11196–11204
- [82] Lin L et al (2016) Surface engineering of copper foils for growing centimeter-sized single-crystalline graphene. *ACS Nano* 10(2):2922–2929
- [83] Li J, Wang X-Y, Liu X, Jin Z, Wang D, Wan L (2015) Facile growth of centimeter-sized single-crystal graphene on copper foil at atmospheric pressure. *J Mater Chem C* 3(15):3530–3535
- [84] Thiele S et al (2010) Engineering polycrystalline Ni films to improve thickness uniformity of the chemical-vapor-deposition-grown graphene films. *Nanotechnology* 21(1):15601
- [85] Edwards RS, Coleman KS (2013) Graphene film growth on polycrystalline metals. *Acc Chem Res* 46(1):23–30
- [86] Ryabchikov IV, Belov BF, Mizin VG (2014) Reactions of metal oxides with carbon. *Steel Transl* 44(5):368–373
- [87] Gottardi S et al (2015) Comparing graphene growth on Cu(111) versus oxidized Cu(111). *Nano Lett* 15(2):917–922
- [88] Hao Y et al (2013) The role of surface oxygen in the growth of large single-crystal graphene on copper. *Science* 342(6159):720–723
- [89] Liang T et al (2015) Graphene nucleation preferentially at oxygen-rich Cu sites rather than on pure Cu surface. *Adv Mater* 27(41):6404–6410
- [90] Son IH et al (2014) CO₂ enhanced chemical vapor deposition growth of few-layer graphene over NiO_x. *ACS Nano* 8(9):9224–9232
- [91] Wu P, Zhang W, Li Z, Yang J (2014) Mechanisms of graphene growth on metal surfaces: theoretical perspectives. *Small* 10(11):2136–2150
- [92] Zhong L et al (2016) Unraveling the influence of metal substrates on graphene nucleation from first-principles study. *J Phys Chem C* 120(40):23239–23245
- [93] Joyner RW, Darling GR, Pendry JB (1988) Stability of bulk and surface carbide layers and their relation to the Fischer-Tropsch hydrocarbon synthesis. *Surf Sci* 205(3):513–522
- [94] Hugosson H (2001) Phase stability diagrams of transition metal carbides, a theoretical study. *Chem Phys Lett* 333(January):444–450
- [95] Zou Z, Fu L, Song X, Zhang Y, Liu Z (2014) Carbide-forming groups IVB-VIB metals: a new territory in the periodic table for CVD growth of graphene. *Nano Lett* 14(7):3832–3839
- [96] Massalski T (1986) Binary alloy phase diagrams. American Society for Metals, Metals Park
- [97] An X, Liu F, Jung YJ, Kar S (2012) Large-area synthesis of graphene on palladium and their Raman spectroscopy. *J Phys Chem C* 116(31):16412–16420
- [98] Losurdo M, Giangregorio MM, Capezzuto P, Bruno G (2011) Graphene CVD growth on copper and nickel: role of hydrogen in kinetics and structure. *Phys Chem Chem Phys* 13(46):20836
- [99] Baraton L et al (2011) On the mechanisms of precipitation of graphene on nickel thin films. *EPL (Europhys Lett)* 96(4):46003
- [100] Niessen AK, De Boer FR (1981) The enthalpy of formation of solid borides, carbides, nitrides, silicides and phosphides of transition and noble metals. *J Less-Common Met* 82:75–80
- [101] Ning J et al (2017) Review on mechanism of directly fabricating wafer-scale graphene on dielectric substrates by chemical vapor deposition. *Nanotechnology* 28(28):284001
- [102] Wang Q, Zhang P, Zhuo Q, Lv X, Wang J, Sun X (2015) Direct synthesis of Co-doped graphene on dielectric substrates using solid carbon sources. *Nano-Micro Lett* 7(4):368–373

- [103] Lee H et al (2016) Nanoscale direct mapping of noise source activities on graphene domains. *ACS Nano* 10(11):10135–10142
- [104] Wang B et al (2016) Direct growth of graphene on gallium nitride using C_2H_2 as carbon source. *Front Phys* 11(2):116803
- [105] Kaplas T, Svirko Y (2014) Self-assembled graphene on dielectric micro- and nanostructures. *Carbon* 70:273–278
- [106] Ueda K, Aichi S, Asano H (2016) Direct formation of graphene layers on diamond by high-temperature annealing with a Cu catalyst. *Diam Relat Mater* 63:148–152
- [107] Kim H et al (2013) Copper-vapor-assisted chemical vapor deposition for high-quality and metal-free single-layer graphene on amorphous SiO_2 substrate. *ACS Nano* 7(8):6575–6582
- [108] Wang D, Tian H, Yang Y, Xie D, Ren TL, Zhang Y (2013) Scalable and direct growth of graphene micro ribbons on dielectric substrates. *Sci Rep* 3:1348-1–1348-7. <https://doi.org/10.1038/srep01348>
- [109] McNerny DQ et al (2014) Direct fabrication of graphene on SiO_2 enabled by thin film stress engineering. *Sci Rep* 4:5049-1–5049-9. <https://doi.org/10.1038/srep05049>
- [110] Muñoz R, Munuera C, Martínez JI, Azpeitia J, Gómez-Aleixandre C, García-Hernández M (2017) Low temperature metal free growth of graphene on insulating substrates by plasma assisted chemical vapor deposition. *2D Mater* 4(1):15009
- [111] Jacob MV et al (2015) Catalyst-free plasma enhanced growth of graphene from sustainable sources. *Nano Lett* 15(9):5702–5708
- [112] Fowlkes JD et al (2006) Control of catalyst particle crystallographic orientation in vertically aligned carbon nanofiber synthesis. *Carbon* 44(8):1503–1510
- [113] Wiltner A, Linsmeier C (2008) Thermally induced reaction and diffusion of carbon films on Ni(111) and Ni(100). *Surf Sci* 602(23):3623–3631
- [114] Wiltner A, Linsmeier C, Jacob T (2008) Carbon reaction and diffusion on Ni(111), Ni(100), and Fe(110): Kinetic parameters from x-ray photoelectron spectroscopy and density functional theory analysis. *J Chem Phys* 129(11):84704
- [115] Ogawa S et al (2013) Graphene growth and carbon diffusion process during vacuum heating on Cu (111)/ Al_2O_3 substrates. *Jpn J Appl Phys* 52:110122
- [116] Moshkalev SA, Verissimo C (2007) Nucleation and growth of carbon nanotubes in catalytic chemical vapor deposition. *J Appl Phys* 102(4):044303-1–044303-6. <https://doi.org/10.1063/1.2769354>
- [117] Elliott JA, Shibuta Y, Amara H, Bichara C, Neyts EC (2013) Atomistic modelling of CVD synthesis of carbon nanotubes and graphene. *Nanoscale* 5(15):6662–6676
- [118] Hofmann S, Csányi G, Ferrari AC, Payne MC, Robertson J (2005) Surface diffusion: the low activation energy path for nanotube growth. *Phys Rev Lett* 95(3):1–4
- [119] Jung DH, Kang C, Nam JE, Jeong H, Lee JS (2016) Surface diffusion directed growth of anisotropic graphene domains on different copper lattices. *Sci Rep* 6:21136
- [120] Stolk PA, Gossmann H-J, Eaglesham DJ, Poate JM (1996) The effect of carbon on diffusion in silicon. *Mater Sci Eng B* 36(1–3):275–281
- [121] Werner P, Gösele U, Gossmann HJ, Jacobson DC (1998) Carbon diffusion in silicon. *Appl Phys Lett* 73(17):2465–2467
- [122] Newman RC, Wakefield J (1961) The diffusivity of carbon in silicon. *J Phys Chem Solids* 19(3–4):230–234
- [123] Kim BS et al (2015) Carbon out-diffusion mechanism for direct graphene growth on a silicon surface. *Acta Mater* 96:18–23
- [124] Scharmann F, Maslarski P, Lehmkuhl D, Stauden T, Pezoldt J (2001) Evaluation of carbon surface diffusion on silicon by using surface phase transitions. *4348: 173–177*
- [125] Yazyev OV, Pasquarello A (2008) Carbon diffusion in CVD growth of carbon nanotubes on metal nanoparticles. *Phys Status Solidi Basic Res* 245(10):2185–2188
- [126] Shin H-A-S et al (2014) Highly uniform growth of monolayer graphene by chemical vapor deposition on Cu–Ag alloy catalysts. *Phys Chem Chem Phys* 16:3087–3094
- [127] Fu Z, Zhang Y, Yang Z (2015) Growth mechanism and controllable synthesis of graphene on Cu–Ni alloy surface in the initial growth stages. *Phys Lett A* 379(20–21):1361–1365
- [128] Wu T et al (2016) Fast growth of inch-sized single-crystalline graphene from a controlled single nucleus on Cu–Ni alloys. *Nat Mater* 15:43–48
- [129] Barin I (2008) Thermochemical data of pure substances. Wiley, New York
- [130] Muñoz R, Gómez-Aleixandre C (2013) Review of CVD synthesis of graphene. *Chem Vap Depos* 19(10–12):297–322